



ЕЛЕКТРОНІКА ТА ІНЖЕНЕРІЯ

OPTIMIZATION OF GEOMETRY OF PIEZORESISTIVE EFFECT ON THE EXAMPLE OF CUBIC CRYSTALS

O. Buryy^[ORCID: 0000-0002-3491-6741], B. Olchovyk, O. Hrinchenko, A. Andrushchak^[ORCID: 0000-0002-8611-3027],
M. Andrushchak

Lviv Polytechnic National University, 12, S. Bandery str., Lviv, 79013, Ukraine

Corresponding author: O. Buryy (e-mail: oleh.a.buryi@lpnu.ua)

(Given 3 February 2024)

On the example of semiconductor crystals Ge, Si, PbTe, PbS, InSb with different levels of doping and different types of conductivity, the geometry of the piezoresistive effect was optimized, namely, such directions of voltage measuring and uniaxial pressure applying were determined, which ensure the maximum achievable value of the effect. The optimization is based on an approach using the construction and analysis of extreme surfaces that represent all possible maxima of the objective function (the magnitude of the effect) under different spatial orientations of interacting factors. The optimization parameters were the angles that determine the directions of the unit vectors of the directions of current and uniaxial pressure applying. The directions of the radius vectors of the points on the extreme surface coincide with the ones in which the electric voltage is measured, and the length of this radius vector for each point was determined by setting such optimization parameters for which the magnitude of the effect for a given direction of voltage measuring would be maximal. It is shown that the optimal interaction geometry in most of the studied cases is longitudinal, and only for n-PbTe, p-InSb crystals it is transverse (although not identical), and the optimal directions for the studied crystals are $\langle 100 \rangle$, $\langle 110 \rangle$ or $\langle 111 \rangle$ depending on the composition of the crystal and the type of doping. Despite the fact that all investigated crystals belong to the same point symmetry group ($m\bar{3}m$), the shapes of the extreme surfaces for them are significantly different, which is caused by different ratios between the piezoresistive coefficients. Typical forms of extreme surfaces have been identified, and in order to explain the obtained results, an analysis of limiting cases that differ in the ratio of piezoresistive coefficients has been carried out. Based on this analysis, four main types of extreme surfaces were established. A scheme has been built that allows, in the case of cubic crystals, to estimate the type of extreme surface and the corresponding optimal directions of voltage measuring, current density (for cubic crystals, these directions coincide) and uniaxial pressure applying. On the basis of this scheme, the forms of extreme surfaces obtained for the investigated crystals are explained.

Keywords: *piezoresistors, sensors, semiconductors, optimization, extreme surfaces*

UDC: 53.06

1. Introduction

As it is known, the piezoresistive effect is the dependence of the resistance of conductors and semiconductors on the mechanical stresses (deformations) applied to them. The piezoresistive effect is used in pressure sensors (electronic scales, blood pressure sensors, etc.), flow sensors, accelerometers,

gyroscopes, transducers, cantilevers of atomic force microscopes, elements of other information and measurement systems. It should be noted that piezoresistive sensors are one of the oldest and most widely used silicon microcircuits [1-3]. The advantages of piezoresistive transducers on such microcircuits include linearity (absence of hysteresis) and high resolution. Piezoresistive sensors are more sensitive to small accelerations than piezoelectric ones, which leads to their widespread use in automotive safety systems (air bags, anti-lock braking systems). Recently, flexible and stretchable electromechanical (in particular, piezoresistive) pressure/strain sensors, particularly based on graphene composites, have also attracted considerable attention [4].

This work is devoted to the problem of determining the maximum achievable value of the piezoresistive effect in crystalline materials, that can be useful both for increasing the efficiency of the devices and evaluating the prospects of using the material to create such devices. The basis of the analysis is the approach previously used by the authors to solve similar problems in the cases of electro-, piezo-, acousto-optical and nonlinear-optical effects (see [5-8] and the works of the authors cited there). According to this approach, such directions of action of the interacting factors are determined (for the piezoresistive effect – the directions in which the electric voltage is measured and compression/tension is applied), in which the magnitude of the effect is the highest. To determine these directions, an optimization procedure is used, the result of which is presented in the form of a special type of surfaces (extreme ones according to the principle of their construction).

2. Basic relations

The piezoresistive effect is defined as a change of the components of the resistivity tensor ρ_{il} under the influence of mechanical stress σ [9]:

$$E_i = \rho_{ik}^0 (\delta_{kl} + \Pi_{klmn} \sigma_{mn}) j_l, \quad (1)$$

where E_i are the components of the electrical field strength, j_l are the components of the current density, σ_{mn} are the components of the mechanical stress tensor, ρ_{ik}^0 are the components of the resistivity tensor at the absence of mechanical stress, Π_{klmn} are the components of the tensor of piezoresistive coefficients, δ_{kl} is the Kronecker symbol, in (1) the summation is performed over repeating indices.

The piezoresistive effect is most strongly manifested in semiconductor materials – Si, Ge, GaSb, InSb, PbTe, Bi₂Te₃, etc., because it occurs both due to a change in the band structure and geometric dimensions of the semiconductor [1, 10]. Sensitive strain gauge devices are realized on the basis of semiconductors, which, however, have such a drawback as the dependence of the measurement results on the surrounding conditions – temperature, radiation, electric and magnetic fields. In practical applications of the piezoresistive effect, the voltage U is measured in the direction of the unit vector \vec{u} , $U = a \vec{E} \vec{u}$, where a is the basis for voltage measuring (at that the piezoresistive sensors are connected, as a rule, according to the Wheatstone bridge scheme). The current density, respectively, is equal to $\vec{j} = \frac{I}{S} \vec{q}$, where \vec{q} is the unit vector of the flow direction, and S is the cross-sectional area of the piezoresistor. Therefore, the relation voltage obtained from (1) is:

$$U = a \frac{I}{S} \rho_{ik}^0 u_i (\delta_{kl} + \Pi_{klmn} \sigma_{mn}) q_l. \quad (2)$$

In the case of uniaxial compression/stretching, the tensor $\sigma = \sigma \vec{s} \vec{s}$, where \vec{s} is the unit vector of the direction of compression/stretching, $\vec{s} \vec{s}$ denotes a tensor dyad. The components of the tensor σ are:

$$\begin{aligned}
\sigma_1 &= \sigma s_1^2 = \sigma \sin^2 \theta_\sigma \cos^2 \varphi_\sigma, \\
\sigma_2 &= \sigma s_2^2 = \sigma \sin^2 \theta_\sigma \sin^2 \varphi_\sigma, \\
\sigma_3 &= \sigma s_3^2 = \sigma \cos^2 \theta_\sigma, \\
\sigma_4 &= \sigma s_2 s_3 = \sigma \sin \theta_\sigma \cos \theta_\sigma \sin \varphi_\sigma, \\
\sigma_5 &= \sigma s_1 s_3 = \sigma \sin \theta_\sigma \cos \theta_\sigma \cos \varphi_\sigma, \\
\sigma_6 &= \sigma s_1 s_2 = \sigma \sin^2 \theta_\sigma \sin \varphi_\sigma \cos \varphi_\sigma.
\end{aligned} \tag{3}$$

where θ_σ , φ_σ are the angles of the spherical coordinate system that determine the direction of uniaxial compression/stretching, σ is a constant value that is equal to the value of the mechanical tension during stretching along Z axis. In (4), a two-index notation system is used (1 \leftrightarrow 11; 2 \leftrightarrow 22; 3 \leftrightarrow 33; 4 \leftrightarrow 23,32; 5 \leftrightarrow 13,31; 6 \leftrightarrow 12,21).

Data on piezoresistive coefficients for some semiconductor crystals studied in this paper are given in Table 1.

Table 1.

Piezoresistive coefficients of studied cubic semiconductor crystals (in $10^{-11} \text{ m}^2/\text{N}$) [9]

Crystal	Π_{11}	Π_{12}	Π_{44}	Crystal	Π_{11}	Π_{12}	Π_{44}
n-Ge1	-4.7	-5.0	-137.9	n-PbTe	20.0	25.0	-107.0
n-Ge2	-2.3	-3.2	-138.1	p-PbTe	35.0	40.0	185.0
p-Ge	-3.7	3.2	96.7	n-PbS	11.6	6.6	11.2
n-Si	-102.2	53.4	-13.6	n-InSb	81.6	114.2	83.0
p-Si	6.6	-1.1	138.3	p-InSb	-70.0	-115.0	-10.0

All the crystals listed in Table 1 belong to the cubic syngony (point group of symmetry $m\bar{3}m$), accordingly, their matrix of piezoresistive coefficients contains only three independent coefficients, and its general form is as follows [1,9]:

$$\Pi = \begin{pmatrix} \Pi_{11} & \Pi_{12} & \Pi_{12} & 0 & 0 & 0 \\ \Pi_{12} & \Pi_{11} & \Pi_{12} & 0 & 0 & 0 \\ \Pi_{12} & \Pi_{12} & \Pi_{11} & 0 & 0 & 0 \\ 0 & 0 & 0 & \Pi_{44} & 0 & 0 \\ 0 & 0 & 0 & 0 & \Pi_{44} & 0 \\ 0 & 0 & 0 & 0 & 0 & \Pi_{44} \end{pmatrix}. \tag{4}$$

Since for cubic crystals the value of resistance in the absence of applied mechanical stress does not depend on the direction, so $\rho_{ik}^0 = \rho_0 \delta_{ik}$ and the expression (2) can be written as

$$U = a \frac{I}{S} \rho_0 |u_l q_l + u_k \Pi_{klmn} \sigma_{mn} q_l|. \tag{5}$$

As can be seen from (5), the maximum effect will be observed at the maximum (modulo) value

$$\Delta = |U - U(\sigma = 0)| = a \frac{I}{S} \rho_0 |u_k \Pi_{klmn} \sigma_{mn} q_l| = a \frac{I}{S} \rho_0 \sigma |u_k \Pi_{klmn} s_m s_n q_l|, \tag{6}$$

which, with given piezoresistive coefficients, depends on the directions of three unit vectors \vec{u} , \vec{q} and \vec{s} ; in turn, each of them is determined by two angles of the spherical coordinate system:

$$\begin{aligned}
u_1 &= \sin \theta_u \cos \varphi_u, & u_2 &= \sin \theta_u \sin \varphi_u, & u_3 &= \cos \theta_u, \\
q_1 &= \sin \theta_q \cos \varphi_q, & q_2 &= \sin \theta_q \sin \varphi_q, & q_3 &= \cos \theta_q, \\
s_1 &= \sin \theta_\sigma \cos \varphi_\sigma, & s_2 &= \sin \theta_\sigma \sin \varphi_\sigma, & s_3 &= \cos \theta_\sigma.
\end{aligned} \tag{7}$$

The anisotropy of the piezoresistive properties of semiconductor crystals is significantly pronounced, as evidenced by the shapes of the indicative surfaces of the longitudinal piezoresistive effect given in [9]. In other words, the magnitude of the effect strongly depends on the orientation of the directions of the listed unit vectors. In order to provide the larger effect desired for piezoresistive devices, their design should be optimized in accordance with these orientations.

To take into account only the directions of the vectors \vec{u} , \vec{q} , \vec{s} , further the coefficient before the module in (6) will be set equal to one, so

$$\Delta = \left| u_k \Pi_{klmn} s_m s_n q_l \right|. \tag{8}$$

We will consider this value as the objective function of the optimization process, which will ensure the achievement of the maximum of Δ .

Note that when the directions of the current density, the voltage measuring and the uniaxial compression/stretching coincide, the longitudinal piezoresistive effect is observed, whereas when one of them is perpendicular to the other two, parallel to each other, a transverse effect occurs.

3. The method of finding the maximum of the piezoresistive effect. Extreme surfaces

As noted above, the objective of this paper is to determine the maxima of the piezoresistive effect on the example of the semiconductor crystals listed in Table 1. The objective function in the optimization is the value of Δ given by expression (8), and the parameters of the optimization, variable in its process, are the angles that determine the directions of the unit vectors \vec{u} , \vec{q} and \vec{s} (or only \vec{q} and \vec{s}).

We searched for the maximum of Δ using the same method that was used in papers [5–8], which is based on the construction of so-called extreme surfaces that reflect all possible maxima of the magnitude of the effect. By analogy with these works, we will construct the extreme surfaces of the piezoresistive effect according to the following algorithm:

1) all piezoresistive coefficients of the material are specified (at the given temperature and other conditions);

2) an array of points is specified at which extreme (maximum) values of Δ will be calculated; the position of each of the points on the surface is determined by the spherical angles θ_u , φ_u , which determine the direction in which the electric voltage is measured;

3) for each point defined in 2), the optimization is carried out according to four parameters (in general case) – the angles θ_q , φ_q , θ_σ , φ_σ , which determine the directions of current density and uniaxial pressure applying. The value Δ_{\max} obtained as a result of optimization determines for a given direction (θ_u , φ_u) the modulus of the radius vector directed from the origin of the coordinate system to a point on the extreme surface;

4) similarly, all other values are found and the extreme surface of the parameter Δ is constructed for all directions of the vector \vec{u} . The extreme surface as a whole represents the dependence $\Delta_{\max}(\theta_u, \varphi_u)$.

From the obtained array of Δ_{\max} values, the global maximum value Δ_{\max}^{extr} for the given surface and the values of the optimal angles θ_u , φ_u , θ_q , φ_q , θ_σ , φ_σ at which it is realized are determined.

All extreme surfaces were built with a step of 1 degree on the angles θ_u and φ_u . Optimization on the angles θ_q , φ_q , θ_σ , φ_σ was carried out by the Levenberg-Marquardt method [11].

4. Results and discussion

Examples of extreme surfaces obtained during optimization on four angles $\theta_q, \varphi_q, \theta_\sigma, \varphi_\sigma$ for semiconductor crystals listed in Table 1 are shown in Fig. 1 (isometric projection and top view), and data on extreme values Δ_{\max}^{extr} and corresponding optimal angles $\theta_u, \varphi_u, \theta_q, \varphi_q, \theta_\sigma, \varphi_\sigma$ are given in Table 2.

As can be seen from the figures, the symmetry of the surfaces corresponds to the symmetry of the crystals (all of them belong to the point group of symmetry $m\bar{3}m$). At the same time, the shapes of the surfaces are different, which is obviously caused by different ratios between the piezoresistive coefficients of the investigated crystals.

The extreme surfaces obtained as a result of the calculation have several typical shapes: the ‘cubic’ shape, similar to the shape of the surface for n-Ge1, n-InSb crystals (Fig. 1), is also obtained for n-Ge2, p-Ge, p-Si, p-PbTe, n-PbS, i.e. for the majority of the crystals listed in Table 1. Among these crystals, n-PbS is characterized by a slightly different, ‘smoothed’ surface (see Fig. 1). The ‘octahedral’ shape of the surface occurs only for one crystal – n-Si (Fig. 1), whereas for n-PbTe, p-InSb a ‘cubo-octahedral’ shape is observed (all the listed polyhedra can be obtained by placing their vertices at the points of the extreme surfaces, the furthest from the origin of the coordinates).

The difference in surface shapes for different crystals is obviously due to the difference in the ratio of their piezoresistive coefficients. Indeed, let’s consider the extreme surfaces for the following limiting cases of the ratio of coefficients:

- | | |
|------------------------------------------|----------------------------------------|
| 1) $ II_{11} \gg II_{12} , II_{44} ;$ | 7) $II_{11} = -II_{44} \gg II_{12} ;$ |
| 2) $ II_{12} \gg II_{11} , II_{44} ;$ | 8) $II_{12} = II_{44} \gg II_{11} ;$ |
| 3) $ II_{44} \gg II_{11} , II_{12} ;$ | 9) $II_{12} = -II_{44} \gg II_{11} ;$ |
| 4) $II_{11} = II_{12} \gg II_{44} ;$ | 10) $II_{11} = II_{12} = II_{44};$ |
| 5) $II_{11} = -II_{12} \gg II_{44} ;$ | 11) $II_{11} = II_{12} = -II_{44};$ |
| 6) $II_{11} = II_{44} \gg II_{12} ;$ | 12) $II_{11} = -II_{12} = II_{44};$ |
| | 13) $-II_{11} = II_{12} = II_{44}.$ |

Conditionally assuming that the value of the ‘large’ coefficients in cases 1) – 13) is $100 \cdot 10^{-11} \text{ m}^2/\text{N}$, and the ‘small’ coefficients are equal to zero, we construct extreme surfaces according to the algorithm given earlier. The corresponding extreme surfaces are shown in Fig. 2.

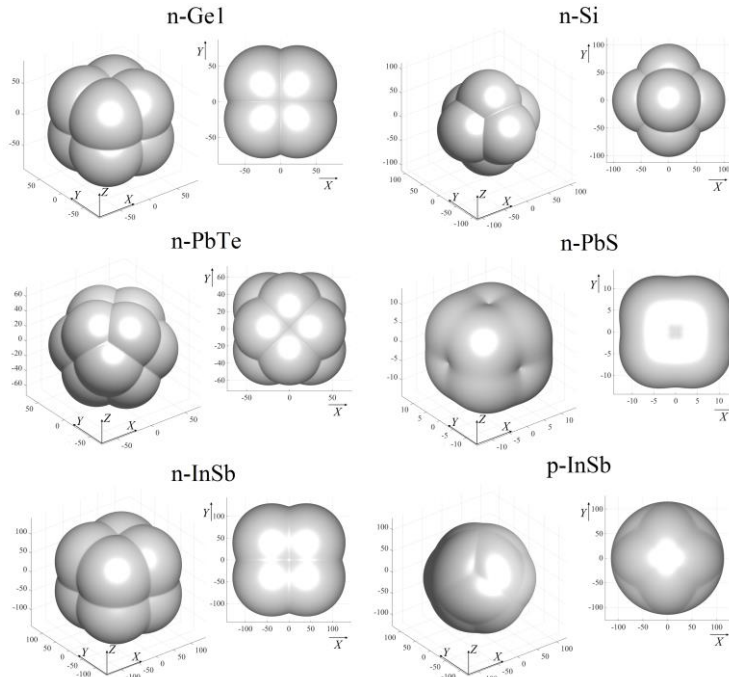


Fig. 1. Examples of extreme surfaces for the investigated crystals (optimization on four angles)

Table 2.

Results of optimization on four angles*

Crystal	θ_u , deg.	φ_u , deg.	θ_q , deg.	φ_q , deg.	θ_σ , deg.	φ_σ , deg.	Δ_{\max}^{extr} , $10^{-11} \text{ m}^2/\text{N}$
n-Ge1	55	45	54.6	45	54.8	45	96.8
n-Ge2	55	45	54.6	45	54.8	45	95.0
p-Ge	55	45	54.6	45	54.8	45	65.4
n-Si	0	–	0	–	0	–	102.2
p-Si	55	45	54.6	45	54.8	45	93.7
n-PbTe	45	0	45	0	45	180	76.0
p-PbTe	55	45	54.7	45	54.8	45	161.7
n-PbS	55	45	54.9	45	54.9	45	15.7
n-InSb	55	45	54.9	45	54.7	45	158.7
p-InSb	45	0	45	0	90	90	115

* To simplify the presentation, the position of only one of the equivalent maxima is given, the positions of the others can be obtained by applying the symmetry elements of the m3m point group.

As it is seen from Fig. 2, the ‘cubic’ extreme surface appears in three cases – the third, eighth, and tenth. The ‘octahedral’ surface appears only once, at $|II_{11}| \gg |II_{12}|, |II_{44}|$, and the ‘cubo-octahedral’ one – three times (cases 2, 7, 11), while in the seventh case it has a smoothed shape, which can be considered as transitional between ‘cubo-octahedral’ or ‘octahedral’ shapes to spherical ones. The latter is implemented in almost half of the limiting cases, at that the radius of the sphere is equal to the value of the non-zero coefficients ($100 \cdot 10^{-11} \text{ m}^2/\text{N}$). This result is easy to obtain analytically by putting, for example, in (7) $II_{11} = II_{12} = II = 100 \cdot 10^{-11} \text{ m}^2/\text{N}$, $II_{44} = 0$. After multiplying and summation in (8), one can obtain that

$$\Delta = \Pi |u_1 q_1 + u_2 q_2 + u_3 q_3| = \Pi |\vec{u} \cdot \vec{q}|, \tag{9}$$

i.e. Δ in this case does not depend on the direction of uniaxial pressure at all. The maximum of Δ will obviously correspond to the maximum of the modulus of the scalar product, which is equal to one for unit vectors. Therefore, $\Delta_{\max} = \Delta$ regardless of the direction of the vector \vec{u} , which means the spherical shape of the extreme surface.

All surfaces shown in Fig. 2 can be represented on the diagram, in which each of them corresponds to the middle of a face, the middle of an edge, or the vertex of a cube with an edge length equal to $200 \cdot 10^{-11} \text{ m}^2/\text{N}$ (taking into account that changing the signs of all II_{ij} does not lead to changes in the shape of the surface, we get 26 vertices, midpoints of edges and midpoints of faces of the cube from the 13 considered limiting cases). In the future, such a scheme (Fig. 3) will be called the ‘cube of extreme surfaces’.

If the piezoresistive coefficients of an arbitrary cubic crystal are multiplied by the coefficient at which the highest of the piezoresistive coefficients would be equal to $100 \cdot 10^{-11} \text{ m}^2/\text{N}$, the corresponding extreme surface will be located on one of the three faces of this cube (multiplying all II_{ij} by the same value does not change, obviously, the shape of the surface). In accordance with the axis to which this face is perpendicular, we will denote it as ‘face II_{11} ’, ‘face II_{12} ’, ‘face II_{44} ’. In accordance with the values of the piezoresistive coefficients, we denote by points on these faces the positions of the extreme surfaces for all studied crystals (Fig. 4).

Comparing the positions of the points on the diagrams of Fig. 4 with the shapes of extreme surfaces for the studied crystals, it is easy to see that for all crystals there is a consistency between the shape of the surface and the position of the point on the corresponding face. Thus, the ‘smoothed’ nature of the extreme surface for n-PbS crystal (Fig. 1) is explained by its position on the II_{11} face almost in the middle of the segment (Fig. 4,a), which connects the ‘cubic’ and spherical surfaces.

In general, the schemes shown in Fig. 4, allow to approximately estimate the optimal directions of the vectors \vec{u} , \vec{q} and \vec{s} for any cubic crystals without calculations – for this, it is enough to approximately determine the position of the extreme surface on one of the faces shown in Fig. 4 (in accordance with known piezoresistive coefficients), and estimate the degree of its closeness to extreme surfaces corresponding to limiting cases.

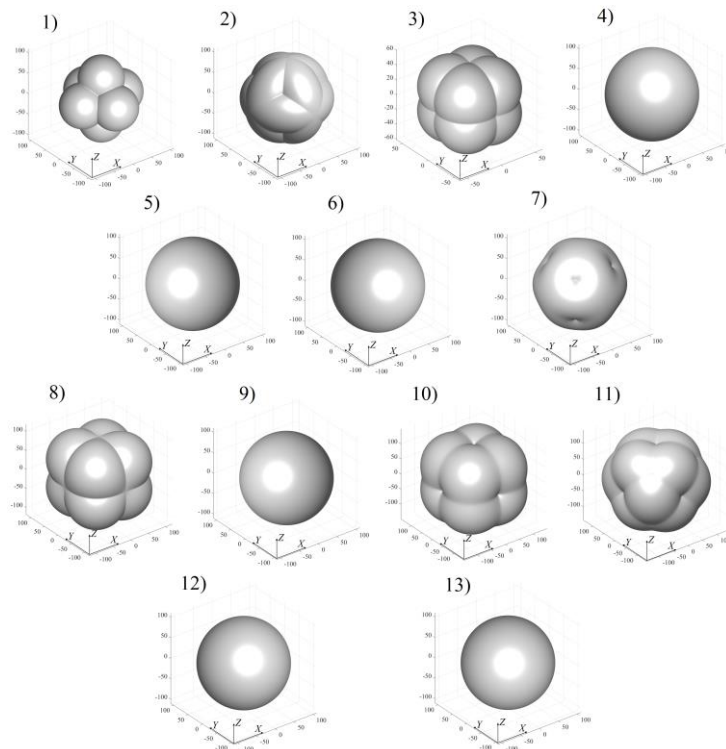


Fig. 2. Extreme surfaces for the limiting cases (optimization on four angles)

The optimal directions for the studied crystals, as can be seen from Table 2, are different for different types of surfaces. Thus, for n-Si crystal ('octahedral' surface), the optimal directions are the directions that coincide with the directions of the $\langle 100 \rangle$ axes, for n-PbTe, p-InSb crystals ('cubo-octahedral' surface) – with the diagonals of the faces of the unit cell $\langle 110 \rangle$, for other crystals – with a volume diagonal of the cube $\langle 111 \rangle$ (the angle $\theta_u = 55^\circ$, specified in Table 2, is an approximate value of the angle between the edge of the cube and its spatial diagonal (54.74°); the approximate nature of this result is due to the fact that extreme surfaces were built with a step of 1 degree on angles θ_u, φ_u).

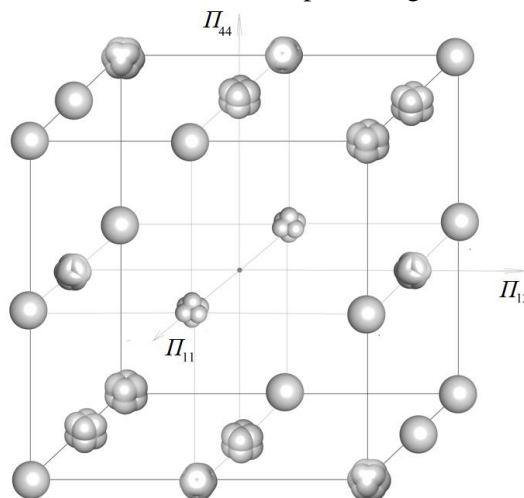


Fig. 3. The 'cube of extreme surfaces'

The optimal geometry of the effect, as can be seen from Table 2, is, within the accuracy of the calculations, longitudinal ($\vec{u} \parallel \vec{q} \parallel \vec{s}$) for the case of crystals with ‘cubo-’ and ‘octahedral’ extreme surfaces, while for crystals with ‘cubo-octahedral’ surfaces (n -PbTe, p-InSb) it is strictly transverse ($\vec{u} \parallel \vec{q} \perp \vec{s}$), although different. Indeed, for n-PbTe the vectors \vec{u} and \vec{s} lie in the same coordinate plane, whereas for p-InSb – in different ones; this result correlates well with the fact that, despite the similarity of the shape of the extreme surfaces, n-PbTe and p-InSb crystals correspond to different faces of the cube of extreme surfaces.

The maximal achievable value Δ_{max}^{extr} can both exceed and be less than the maximum of the coefficients Π_{ij} . As it follows from the comparison of the data given in Tables 1,2, the condition $\Delta_{max}^{extr} \geq \Pi_{ij_{max}}$ is valid for crystals in which the values of different Π_{ij} coefficients are commensurate (n-Si, n-PbS, n-InSb, p-InSb).

As could be expected based on the coefficients given in Table 1, the most significant effect occurs in p-PbTe crystal ($\Delta_{max}^{extr} = 161.7 \cdot 10^{-11} \text{ m}^2/\text{N}$).

As can be seen from Table 2, the vectors \vec{u} and \vec{q} in all considered cases must be parallel (within the accuracy of the calculations). Similarly to the previous one, we will carry out the optimization by setting $\theta_u = \theta_q$, $\varphi_u = \varphi_q$, that is, considering only the angles θ_σ , φ_σ as optimization parameters. Its results are given in Table 3, and the corresponding extreme surfaces are shown in Fig. 5 (for the same crystals as in Fig. 1).

The extreme surfaces shown in Fig. 5, are generally similar to those in Fig. 1, and retain the ‘cubic’, ‘octahedral’ and ‘cubo-octahedral’ shapes. The analysis using the scheme of the cube of extreme surfaces and its faces is also possible these surfaces.

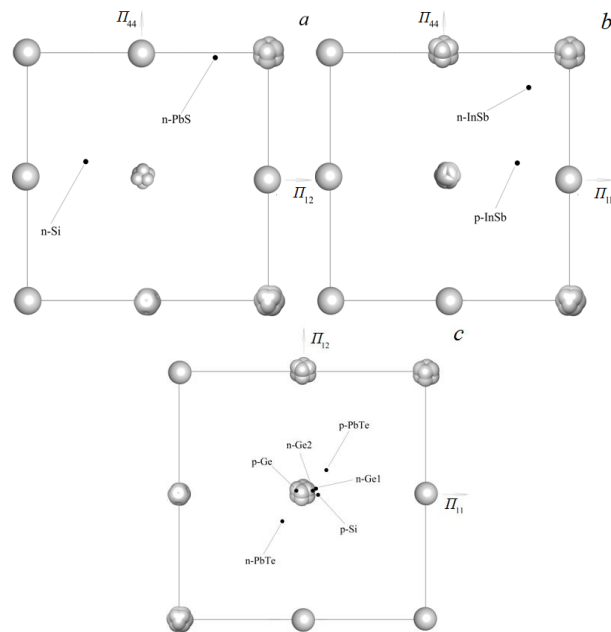


Fig. 4. The faces Π_{11} (a), Π_{12} (b), Π_{44} (c) of the ‘cube of extreme surfaces’ and the points corresponding to investigated crystals

Table 3.

Results of optimization on two angles*

Crystal	θ_u , deg.	φ_u , deg.	θ_σ , deg.	φ_σ , deg.	Δ_{max}^{extr} , $10^{-11} \text{ m}^2/\text{N}$
n-Ge1	55	45	54.8	45	96.8
n-Ge2	55	45	54.8	45	95.0

p-Ge	55	45	54.8	45	65.4
n-Si	0	–	0	–	102.2
p-Si	55	45	54.8	45	93.7
n-PbTe	45	0	45	180	76.0
p-PbTe	55	45	54.8	45	161.7
n-PbS	45	0	45	0	14.7
n-InSb	55	45	54.8	45	158.7
p-InSb	45	0	90	90	115

The maximum achievable values of $\Delta_{\max}^{\text{extr}}$, obtained by the optimization on four and two angles, are the same, which could be expected, based on the high symmetry of all considered crystals. For crystals of lower and middle symmetry categories, however, the situation can be more complicated, which is why in this paper it was considered appropriate to carry out an analysis for the general (four-angle) case. It should also be noted that the use of an approach similar to the one developed here for crystals of lower symmetry will be complicated due to a higher number of independent piezoresistive coefficients. Thus, the presentation of crystals on a scheme similar to the one shown in fig. 4, will require the use of separate sections of the ‘hypercube of extreme surfaces’, which will make the solution of such a problem more cumbersome and will require the development of specialized software for its solution.

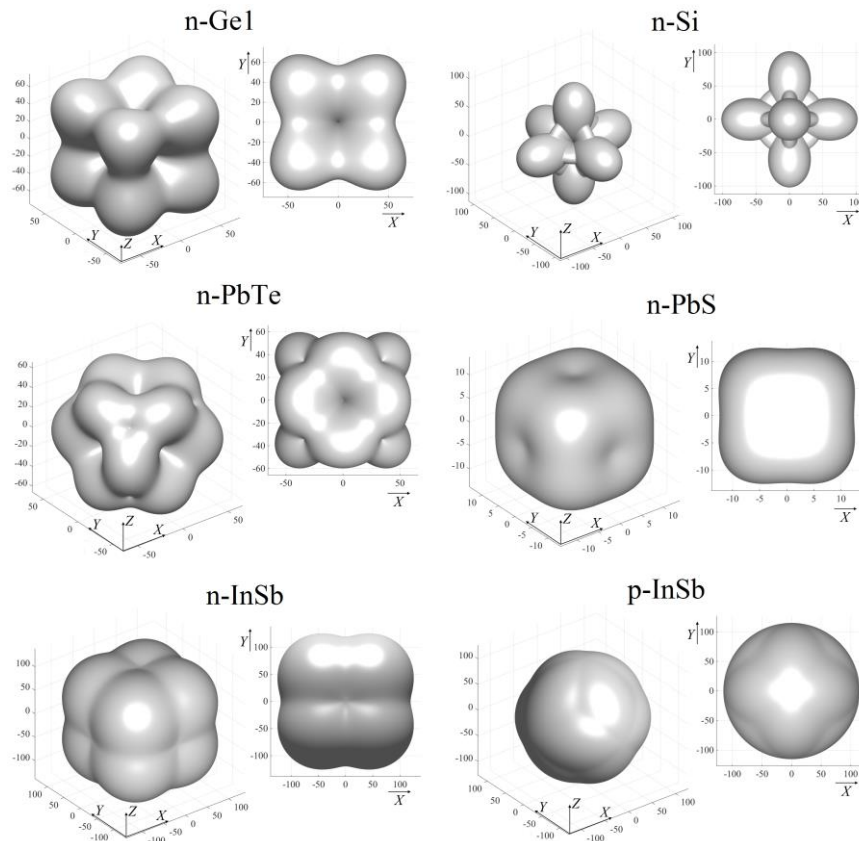


Fig. 5. Examples of extreme surfaces for the investigated crystals (optimization on two angles)

Conclusions

On the example of a number of semiconductor crystals (Ge, Si, PbTe, InSb of n- and p-conductivity types, PbS of n-type conductivity), the geometry of the piezoresistive effect was optimized using the method of extreme surfaces. The directions of voltage measuring \vec{u} , current density \vec{q} , and uniaxial pressure applying \vec{s} which ensure the maximal value of the effect are determined.

It is shown that despite the fact that all the investigated crystals belong to the same point group of symmetry ($m\bar{3}m$), the shape of the extreme surfaces, and, accordingly, the geometries in which the maximal effect is achieved, are significantly different, which is caused by different ratios between the piezoresistive coefficients Π_{ij} . Thus, for n-Si crystal, the optimal directions of \vec{u} , \vec{q} and \vec{s} coincide with the $\langle 100 \rangle$ directions, for n-PbTe, p-InSb crystals – with $\langle 110 \rangle$ ones, for other crystals – with $\langle 111 \rangle$ ones. The optimal geometry of the effect in most of the investigated cases is longitudinal ($\vec{u} \parallel \vec{q} \parallel \vec{s}$), but for n-PbTe, p-InSb crystals it is transverse ($\vec{u} \parallel \vec{q} \perp \vec{s}$). At that the maximal achievable value of the magnitude of the effect can both exceed and be less than the maximum of the piezoresistive coefficients for a given crystal.

In order to identify all possible forms of extreme surfaces, an analysis of limiting cases that differ among themselves in the ratio of piezoresistive coefficients was carried out. On the basis of this analysis, four main types of extreme surfaces - spherical, ‘cubic’, ‘octahedral’ and ‘cubo-octahedral’ were obtained, and a diagram was built that allows to estimate the type of extreme surface and the associated optimal directions of uniaxial pressure applying and voltage measuring for cubic crystals.

In general, the results presented in the work have, first of all, methodological significance, since the presented method of analysis can be applied not only to well-studied semiconductor crystals – Si, Ge, PbTe, PbS, InSb, but also to other materials and other crystal-physical effects.

This research was supported by the Ministry of Education and Science of Ukraine within the framework of state budget projects DB/Nanoarchitectonics and DB/Nanoelectronics (registration number: 0123U101695).

References

- [1] Barlian, A., Park, W.-T., Mallon, J., Rastegar, A. and Pruitt, B. (2009) "Review: Semiconductor piezoresistance for microsystems", *Proc. IEEE*, vol. 97, no. 3, pp. 513-552. doi: 10.1109/JPROC.2009.2013612
- [2] Doll, J. and Pruitt, B. (2013) *Piezoresistor Design and Applications*. Springer Science+Business Media, New York. doi: 10.1007/978-1-4614-8517-9
- [3] Fiorillo, A., Critello, C. and Pullano S. (2018) "Theory, technology and applications of piezoresistive sensors: A review", *Sensors and Actuators A*, vol. 281, pp. 156-175. doi: 10.1016/j.sna.2018.07.006
- [4] Li, J., Fang, L., Sun, B., Li, X. and Kang S. (2020) "Review – Recent progress in flexible and stretchable piezoresistive sensors and their applications", *Journal of The Electrochemical Society*, vol. 167, no. 3, 037561. doi: 10.1149/1945-7111/ab6828
- [5] Buryy, O., Andrushchak, A., Kushnir, O., Ubizskii, S., Vynnyk, D., Yurkevych, O., Larchenko, A., Chaban, K., Gotra, O. and Kityk, A. (2013) "Method of extreme surfaces for optimizing the geometry of acousto-optic interactions in crystalline materials: Example of LiNbO₃ crystals", *J. Appl. Phys.*, vol. 113, no. 8, 083103. doi: 10.1063/1.4792304
- [6] Buryy, O., Andrushchak, A., Demyanyshyn, N. and Mytsyk B. (2016) "Optimizing of piezo-optic interaction geometry in SrB₄O₇ crystals", *Optica Applicata*, vol. 46, no. 3, pp. 447-459. doi: 10.5277/oa160311
- [7] Andrushchak, A., Buryy, O., Andrushchak, N., Hotra, Z., Sushynskiy, O., Singh, G., Janyani, V. and Kityk, I. (2017) "General method of extreme surfaces for geometry optimization of the linear electro-optic effect on an example of LiNbO₃:MgO crystals", *Appl. Opt.*, vol. 56, no. 22, pp. 6255-6262. doi: 10.1364/AO.56.006255
- [8] Andrushchak, N., Buryy, O., Danylov, A., Andrushchak, A. and Sahraoui, B. (2021) "The optimal vector phase matching conditions in crystalline materials determined by extreme surfaces method: Example of uniaxial nonlinear crystals", *Opt. Mat.*, vol. 120, 111420. doi: 10.1016/j.optmat.2021.111420
- [9] Sirotnin, Yu. and Shaskolskaja, M. (1983) *Fundamentals of crystal physics*. Imported Pubn., Moscow.
- [10] *Microelectronic sensors of physical values* (2003). Ed. by Z. Hotra. Vol. 2. Liga-press, Lviv (in Ukrainian).
- [11] Press, W., Flannery, B., Teukolsky, S. and Vetterling, W. (1989) *Numerical Recipes in Pascal. The art of Scientific Computing*. Cambridge University Press, Cambridge.

ОПТИМІЗАЦІЯ ГЕОМЕТРІЇ П'ЄЗОРЕЗИСТИВНОГО ЕФЕКТУ НА ПРИКЛАДІ КУБІЧНИХ КРИСТАЛІВ

О. Бурій, Б. Ольховик, О. Грінченко, А. Андрущак, М. Андрущак

Національний університет «Львівська політехніка» вул. С. Бандери, 12, 79013, Львів, Україна

На прикладі напівпровідникових кристалів Ge, Si, PbTe, PbS, InSb з різними рівнями легування та різними типами провідності проведено оптимізацію геометрії п'єзореzystивного ефекту, а саме визначено такі напрямки вимірювання напруги та прикладання одновісного тиску, які забезпечують максимально досяжне значення ефекту. Оптимізація базується на підході, що використовує побудову та аналіз екстремальних поверхонь, які представляють усі можливі максимуми цільової функції (величини ефекту) при різних просторових орієнтаціях взаємодіючих факторів. Параметрами оптимізації були кути, що визначають одиничні вектори напрямків протікання струму та прикладання одновісного тиску. Напрямок радіус-вектора точок екстремальної поверхні відповідав напрямку, в якому вимірюється електрична напруга, а довжина цього радіус-вектора для кожної точки визначалася шляхом встановлення таких параметрів оптимізації, за яких величина ефекту для даного напрямку є максимальною. Показано, що оптимальна геометрія взаємодії в більшості досліджуваних випадків є поздовжньою, і лише для кристалів n-PbTe, p-InSb вона поперечна (хоча й не тотожна), а оптимальними напрямками для досліджених кристалів є $\langle 100 \rangle$, $\langle 110 \rangle$ або $\langle 111 \rangle$ залежно від складу кристала та типу легування. Незважаючи на те, що всі досліджені кристали належать до однієї точкової групи симетрії ($m\bar{3}m$), форми екстремальних поверхонь для них суттєво відрізняються, що зумовлено різними співвідношеннями між п'єзореzystивними коефіцієнтами. Визначено типові форми екстремальних поверхонь, для пояснення отриманих результатів проведено аналіз граничних випадків, які відрізняються співвідношенням п'єзореzystивних коефіцієнтів. На основі цього аналізу було встановлено чотири основні типи екстремальних поверхонь. Побудовано схему, яка дозволяє для кубічних кристалів оцінити тип екстремальної поверхні та відповідні їй оптимальні напрямки вимірювання напруги, протікання струму (для кубічних кристалів ці два напрямки збігаються) та прикладання одновісного тиску. На основі цієї схеми пояснено форми екстремальних поверхонь, отримані для досліджених кристалів.

Ключові слова: *п'єзореzystори, сенсори, напівпровідники, оптимізація, екстремальні поверхні*